

Mechanical and magnetocaloric adjustable properties of Fe_3O_4/PET deformed nanoparticle film

Fengguo Fan(范凤国) and Lintong Duan(段林彤)
Citation: Chin. Phys. B, 2024, 33 (**3**): 037502. DOI: 10.1088/1674-1056/acf280
Journal homepage: http://cpb.iphy.ac.cn; http://iopscience.iop.org/cpb

What follows is a list of articles you may be interested in

Out-of-plane weak ferromagnetism at room temperaturein lattice-distortion non-collinear antiferromagnet of single-crystal Mn_3Sn

Bo-Xi Zhang(张博熙), Ping Song(宋平), Shan-Shan Deng(邓珊珊), Li Lou(娄理), and Sen Yao(姚森)
Chin. Phys. B, 2023, 32 (**8**): 087502. DOI: 10.1088/1674-1056/acca0b

Bending sensor based on flexible spin valve

L I Naumova, R S Zavornitsyn, M A Milyaev, N G Bebenin, A Y Pavlova, M V Makarova, I K Maksimova, V V Proglyado, A A Zakharov, and V V Ustinov
Chin. Phys. B, 2023, 32 (**5**): 057502. DOI: 10.1088/1674-1056/ac8923

Texture analysis of ultra-high coercivity Sm_2Co_7 hot deformation magnets

Qiang Ma(马强), Meishuang Jia(贾美爽), Zhifeng Hu(胡智峰), Ming Yue(岳明), Yanli Liu(刘艳丽), Tongyun Zhao(赵同云), and Baogen Shen(沈保根)
Chin. Phys. B, 2021, 30 (**4**): 047505. DOI: 10.1088/1674-1056/abe2fc

Close-coupled nozzle atomization integral simulation and powder preparation using vacuum induction gas atomization technology

Peng Wang(汪鹏), Jing Li(李静), Xin Wang(王欣), Heng-San Liu(刘恒三), Bin Fan(范斌), Ping Gan(甘萍), Rui-Feng Guo(郭瑞峰), Xue-Yuan Ge(葛学元), and Miao-Hui Wang(王淼辉)
Chin. Phys. B, 2021, 30 (**2**): 027502. DOI: 10.1088/1674-1056/abc167

Rare earth permanent magnets prepared by hot deformation process

Ren-Jie Chen(陈仁杰), Ze-Xuan Wang(王泽轩), Xu Tang(唐旭), Wen-Zong Yin(尹文宗), Chao-Xiang Jin(靳朝相), Jin-Yun Ju(剧锦云), Don Lee(李东), A-Ru Yan(闫阿儒)
Chin. Phys. B, 2018, 27 (**11**): 117504. DOI: 10.1088/1674-1056/27/11/117504

Mechanical and magnetocaloric adjustable properties of Fe_3O_4/PET deformed nanoparticle film

Fengguo Fan(范凤国)[†] and Lintong Duan(段林彤)

School of Physics and Electrical Information, Shangqiu Normal University, Shangqiu 476000, *China*

(Received 16 March 2023; revised manuscript received 18 August 2023; accepted manuscript online 22 August 2023)

The flexibility of nanoparticle films is a topic of rapidly growing interest in both scientific and engineering researches due to their numerous potential applications in a broad range of wearable electronics and biomedical devices. This article presents the elucidation of the properties of nanoparticle films. Here, a flexible film is fabricated based on polyethylene terephthalate (PET) and magnetic iron oxide at the nanoscale using layer-by-layer technology. The 2D thin flexible film material can be bent at different angles from 0° to 360°. With an increase in elastic deformation angles, the magnetocaloric effect of the film gradually increases in the alternating magnetic field. The test results from a vibrating sample magnetometer and a low-frequency impedance analyzer demonstrate that the film has a good magnetic response and anisotropy. The magnetocaloric effect and magnetic induction effect are controlled by deformation, providing a new idea for the application of elastic films. It combines the flexibility of the nanoparticle PET substrate and, in the future, it may be used for skin adhesion for administration and magnetic stimulation control.

Keywords: nanoparticle film, deformation, magnetic properties, flexible substrates

PACS: 75.30.Gw, 75.30.Kz, 75.50.Ee, 75.75.Jn **DOI:** 10.1088/1674-1056/acf280

1. Introduction

Flexible or stretchable nanoparticle films have been expanding rapidly for many years as they promise mechanical properties for functional and conformable materials that can be applied to research fields such as wearable electronic devices and biomedical devices.[1–6] For example, flexible metallic-oxide-barrier magnetic tunnel-junction devices applied in the flexible electronics field exhibit reliable and stable operation under substantial deformation of the flexible substrates.[7] Increasing numbers of applications are based on the stretchability and flexibility of substrates used for functional nanomaterials. Understanding the mechanical deformation and its effect on the physical properties, tensile and compressive of strains of substrates has received significant interest due to their superior properties.[8,9] Furthermore, the composition of the film surface, with an elastic substrate as the carrier, is also the focus of research.

Magnetic nanomaterials are important components of thin films due to their real-world applications, such as magnetic sensors, magnetic resonance imaging, and biological and medical technology.[10–12] In particular, with regard to well-modified iron oxide nanoparticles, which have good biocompatibility and stability,[13–15] the clinical translation of magnetic nanoparticles composed of iron-oxide-core nanomaterials and a dextran shell has been approved by the FDA for use as nanodrugs in the human body.[16] The combination of flexible substrates and medicinal magnetic nanoparticles provides a biomedicine with practical applications for the assembled nanoparticle films.

In this work, we present a film fabricated using a flexible PET substrate and Fe_3O_4 nanoparticles via LBL technology. The thin film surface was probed by SEM and atomic force microscopy (AFM) during or before bending tests to clearly characterize and identify mechanisms. Due to Raman spectroscopy and contact angle measurement instrument detection techniques, it is possible to explore the optical properties and hydrophilicity of the film surface. Then, a 2D flexible nanoparticle film was bent to different angles from 0° to 360°, and the magnetocaloric effect of the film that gradually increased in the alternating magnetic field was measured. The magnetoelastic and magnetic anisotropy properties of the nanoparticle film were observed experimentally by a vibrating sample magnetometer and a static magnetic field. Finally, the conductivity of the film results was measured by a low-frequency impedance analyzer, which further demonstrated that an ordered magnetic moment part enhances the conductivity of the film. The magnetocaloric effect and magnetic induction effect are controlled by deformation, which provides new applications of biological iron oxide nanoparticles on an elastic substrate.

2. Results and discussion

Recent developments in experimental techniques have shown that size and morphology can affect the properties of nanomaterials[17] Our preliminary work also proved that the fabrication of microstructures can control the properties of composite materials containing functional nanoparticles.[18] Based on this analysis, morphological images of the syn-

[†]Corresponding author. E-mail: fanfengguo@126.com

© 2024 Chinese Physical Society and IOP Publishing Ltd

thesized Fe_3O_4 nanoparticles with transmission electron microscopy (TEM) are shown in Fig. 1(a). The average statistical diameter of the individual nanoparticles is about 14 nm. It is also seen that the nanoparticles, after drying on a silicon wafer, aggregated into clusters, and the scanning electron microscopy (SEM) images are shown in Fig. 1(b). In the experiment, the agglomeration characteristics of nanoparticles were analyzed by nanoparticle tracking analysis, as shown in Figs. 1(c) and 1(d). From these, it can be seen that the aggregation increases with the increase in nanoparticle concentration. The average particle size of nanoparticle agglomeration is 198 nm, and the solution concentration is 5.61×10^8 particles/ml. The spontaneous aggregation of nanoparticles in solution was conducive to our further assembly.

In our experiment, a PET-based flexible Fe_3O_4 nanoparticle film was fabricated using LBL assembly technology, the process of which is schematically described in the experimental section. Figure 2(a) shows the finished assembly product and assembly diagram sketch. The flexible film is mainly composed of an upper layer of nanoparticles Fe_3O_4 and a lower layer of polyethylene terephthalate. As shown in Fig. 1(a), the sample can be bent and deformed at a large angle without damage. To understand the structure composition of the nanoparticle film, the cross section and surface of the film were observed by SEM. The cross-sectional view shows that the thickness of the lower-layer flexible PET material is about 24.12 μm (Fig. 2(b)). The assembly thickness of the upper-layer nanoparticles is about 391.8 nm, as shown in Fig. 2(c). Figures 2(c) and 2(b) also show that the nanoparticles can be tightly attached to the flexible PET substrate after assembly. A photograph and detailed surface characterization of the fabricated film are shown in Figs. 2(d) and 2(f), respectively. SEM images of films fabricated with an approximately 60-layer assembly are shown in Fig. 2(d), where the surface of the nanoparticle film appears compact and homogeneous macroscopically. With the increase in magnification, cluster particle agglomeration on the assembly surface can be found in Figs. 2(e) and 2(f). Firstly, the addition of PDDA solvent can promote dense layer-by-layer bonding between particles; secondly, it also affects the formation of surface clusters of particles.

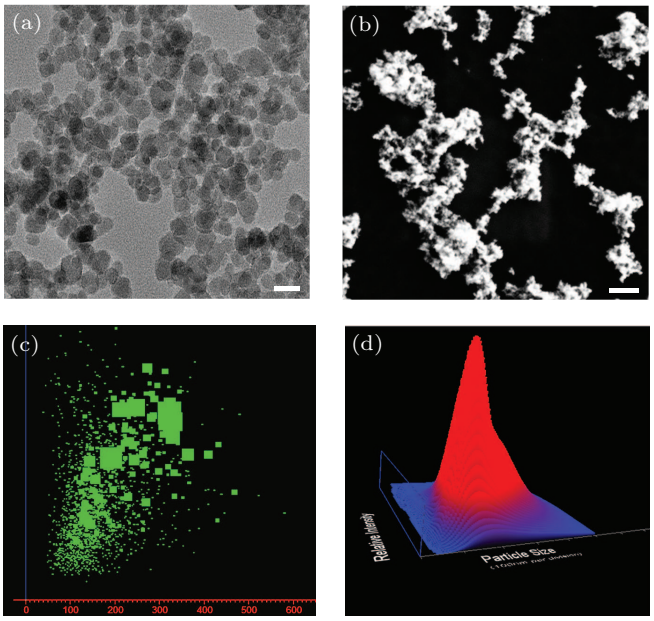


Fig. 1. (a) TEM characterization of Fe_3O_4 nanoparticles (bar: 20 nm). (b) SEM characterization of Fe_3O_4 nanoparticles (bar: 200 nm). (c) Nanoparticle tracking analysis of particle size and relative intensity. (d) A 3D plot of nanoparticle tracking analysis of particle size and relative intensity.

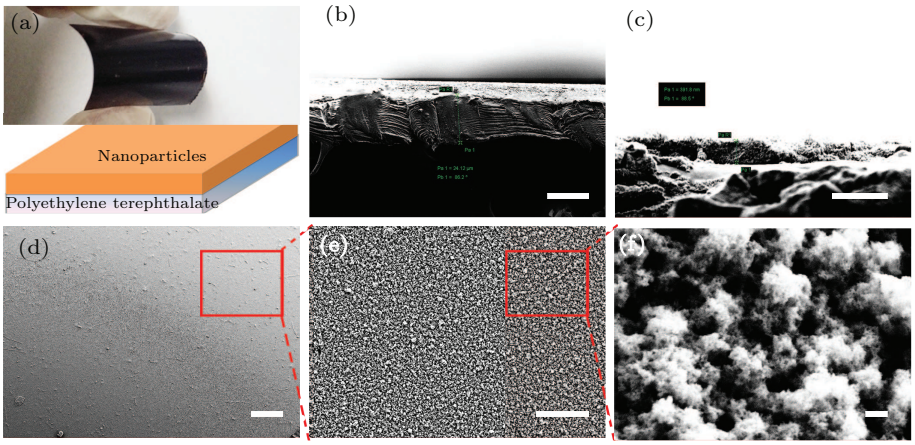


Fig. 2. (a) The physical object and an assembly diagram of an assembled film. (b) An SEM characterization cross-section of the nanoparticle-film-based PET (bar: 20 μm). (c) An SEM characterization cross-section of the Fe_3O_4 nanoparticle (bar: 1 μm). (d) SEM characterization of the flexible nanoparticle film surface (bar: 100 μm). (e) SEM characterization of the flexible nanoparticle film surface (bar: 10 μm). (f) SEM characterization of the flexible nanoparticle film surface (bar: 200 nm).

The AFM measurements also confirmed that the magnetism of nanoparticles increased with aggregation on the surface, as shown in Fig. 3(a). Local amplification and the 3D cross-section of the nanoparticle film stereogram indicated that it consisted of clusters of nanoparticles with a slightly fluctuating surface, averaging about 60 nm, as shown in Fig. 3(b). The slight undulation of the surface was due to the coupling of magnetic nanoparticles during self-assembly.

Raman scattering has led to advancements in the study of the optical properties of metallic nanoparticles. Here, the PET substrate and Fe_3O_4/PET assembled film were detected by Raman scattering in Fig. 3(c). The assembled films had no Raman enhancement effects. In Fig. 3(d), the Raman spectra of three random points on the film surface were measured, from which we can conclude that magnetic nanoparticles are equidistributed on the surface of the film, and the Fe_3O_4/PET assembled film has certain light absorption. The contact angle measurement instrument detected raw untreated and plasma-treated PET substrates in Figs. 3(e) and 3(f), respectively. The contact angles of PET-based films before and after surface treatment were 45.4° and 24.3°, respectively. This proved that the elastic film PET substrate has good hydrophilicity after plasma treatment, and it is more conducive to the assembly of particles on the surface. In Fig. 3(g), after the particles were assembled on the film surface, the contact angles became 26.1°. This indicates that the flexible nanoparticle film has good hydrophilicity, which can be applied to the surface of hydrophilic materials in the future.

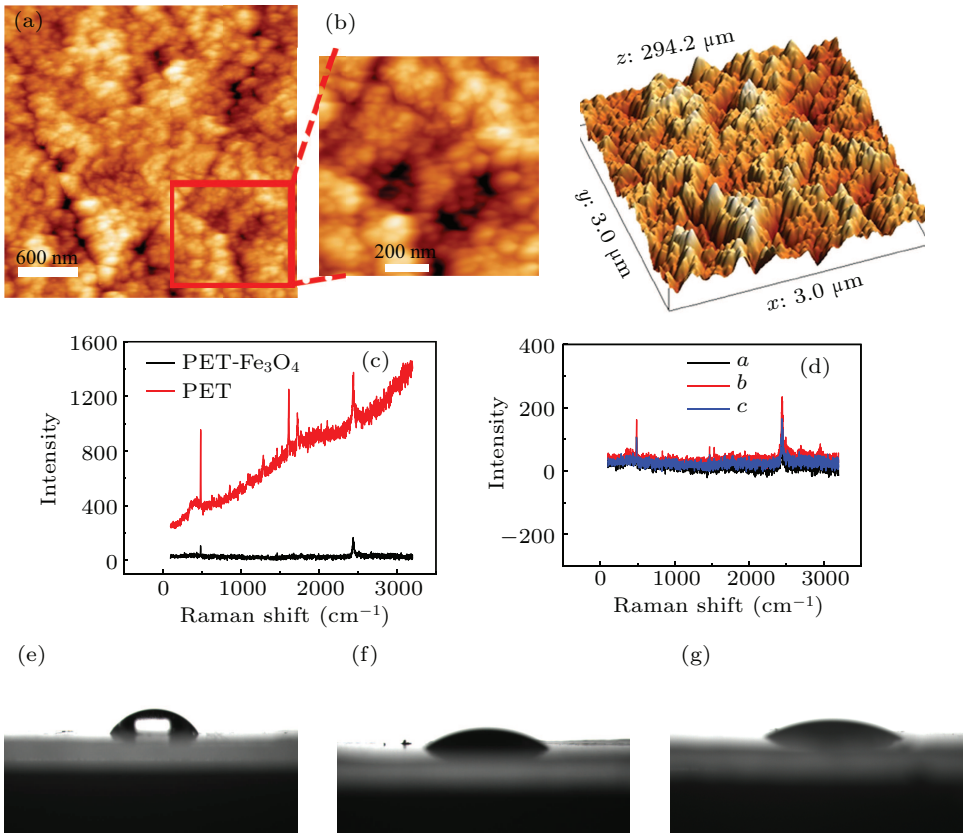


Fig. 3. (a) AFM observation amplitude image results of the Fe_3O_4/PET film surface (bar: 600 nm). (b) A zoomed-in image (bar: 200 nm) and 3D cross section of the nanoparticle film based on PET. (c) Comparison of Raman detection between the assembled Fe_3O_4/PET film and PET substrate. (d) Raman detection of random points on the film surface. (e) The contact angle measurement instrument detecting the PET substrate. (f) The contact angle measurement instrument detecting the substrate after plasma treatment. (g) The contact angle measurement instrument testing the assembly film.

Via plasma surface treatment, the surface of the material is etched and made rough, or a dense cross-linked layer is formed, or oxygen-containing polar groups are introduced to improve its hydrophilicity. Magnetic nanoparticles are then assembled on the surface via electrostatic adsorption, making the particles water-soluble, and the layers are attached to the surface of the PET material. Consequently, after assembly, the contact angle increases, indicating excellent water solubility.

Using vibrating sample magnetometer (VSM) detection in thin films and nanostructures, it is possible to study the magneto-mechanical coupling of flexible magnetic systems and to characterize their dynamic magnetic properties.[19] To study the magnetic properties of Fe_3O_4/PET nanoparticle film, the hysteresis loops were measured at room temperature with a magnetic field applied (as seen in Fig. 4(a)). In the experiment, we observed that the temperature of the film changed with the bending angle under an alternating magnetic field. The film consists of PET substrate and magnetic nanoparticles. We noted that the interaction between the PET substrate and the alternating magnetic field does not generate heat. The root cause of the heat generation is the interaction between the magnetic nanoparticles and the alternating magnetic field and the interaction between the particles themselves. The film is relatively thin compared to the thickness of the substrate, and the particle surface characterization indicates that it remains undamaged, even under deformation of the PET substrate. The deformation and pressure generated in the particles are not the direct causes of temperature changes. Instead, they affect the

interaction area between the alternating magnetic field and the particles, resulting in significant temperature differences under bending. Upon observation, we found that the nanoparticles were superparamagnetic. This is mainly determined by the small nanoparticle size, with each nanoparticle being regarded as a magnetic moment. The hysteresis loop for the field applied parallel to the film is relative to the saturation magnetization of 75 emu/g. When the field is applied perpendicular to the film, the saturation magnetization becomes 68 emu/g. When the applied magnetic field and the film form an angle of 45°, the magnetic saturation magnetization of the film becomes 63 emu/g. These results demonstrate the anisotropy of the nanoparticle film as a result of the external applied magnetic field after assembly. To further verify our results, we dissolved the magnetic particles from the nanoparticle film with hydrochloric acid and dried them for VSM measurement. As shown in Fig. 4(b), the saturation magnetization of the particles was 64 emu/g and did not show any anisotropy. The results also showed that the assembled film could enhance the saturation magnetization. This was mainly due to the orderly arrangement of particles on the surface of the film. This characteristic also provides us with a new idea for the creation of electronic devices.

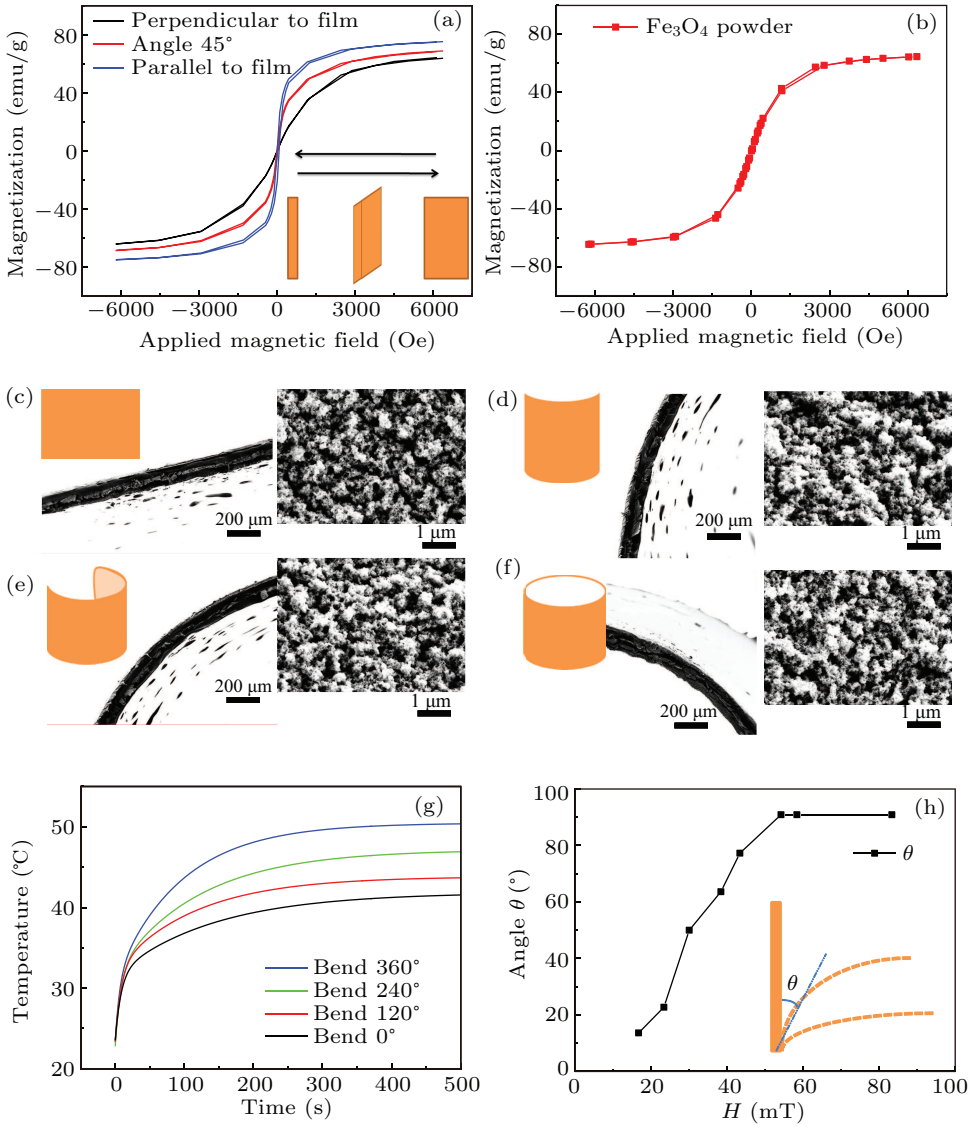


Fig. 4. (a) Hysteresis loops for Fe_3O_4 nanoparticles measured by a vibrating sample magnetometer. (b) Hysteresis loops for Fe_3O_4/PET film obtained under various external magnetic field directions. (c)–(f) SEM characterization of the film surface and local under bending angles of 0°, 120°, 240° and 360°, respectively. (g) Magnetothermal measurements of an assembled film with the different bending deformations (0°, 120°, 240° and 360°). (h) The magnetoelasticity of the film.

Due to the deformability of PET substrates, the stress deformation can be applied to the Fe_3O_4/PET nanoparticle film by inward bending. The magnetic properties are sensitive to the external mechanical stress. Firstly, we characterized the morphology of the films under stress. SEM characterization of the film surface locally under bending angles of 0°, 120°, 240° and 360° is shown in Figs. 4(c)–4(f), respectively. The curvature radius of the material at different angles was computed by bending a 2 cm long and 1 cm wide particle film on a PET substrate along its long surface, using the curva-

ture radius calculation formula $0.02 = R\theta$. Here, R denotes the curvature radius and θ represents the bending angle. The corresponding curvature radii at 0°, 120°, 240° and 360° can be obtained, which are $3/\pi$; $3/2\pi$ and $1/\pi$, respectively. The unit of measurement is centimeters. It can be seen from the figure that the film can bend to a certain angle under the action of stress. The locally enlarged image shows that the surface of the film is not damaged due to deformation. The LBL-assembled films of Fe_3O_4/PET with different bending degrees were subjected to an alternating magnetic field of 390 kHz and the thermogenesis was measured using an optical thermometer. The experimental results are shown in Fig. 4(g). It can be seen that the thermogenesis of the flexible films was dependent on the bending degree when an alternating magnetic field was applied. When the film was bent into a cylindrical shape (360°) and placed in an alternating magnetic field, the temperature measurement results displayed the largest value. When the film was placed in an alternating magnetic field without deformation (0°), the temperature measurement results displayed the smallest value. Here, the energy temperature measurement curve of the film can be explained by the energy absorption cross-section theory. The energy absorption cross-section can be expressed as[20]

$$\sigma = 4\pi\omega V\left(\alpha_{\mathrm{e}} + \alpha_{\mathrm{m}}\right)/c, \tag{1}$$

where σ is the cross-sections of absorption, ω is the angle frequency of the alternating magnetic field, V is the volume of nanoparticles, α_{e}, α_{m} are the imaginary parts of the electric and magnetic polarizability of the particle, respectively, and c is the velocity of light in vacuum. When the film deforms from a plane to a cylinder, the total projected area increases in the magnetic field. After deformation, the effective projected area of the film in the magnetic field increases, resulting in an enhancement of the magnetocaloric effect. Thus, the magnetothermogenic effect can be regulated by the projected area of the deformed film. Our experiment showed that a certain amount of bending did not hinder the attachment of particles to the substrate's surface, as revealed by SEM analysis. However, we also found that the electrostatic attraction and interaction forces between particles were weak, leading to particle detachment during multiple bending. In the experiment, the temperature was kept under 50 °C,[21] which helped to prevent the substrate from fracturing due to high temperatures. Careful temperature control is essential when conducting experiments to ensure accurate and reliable results.

Due to the magnetoelasticity of Fe_3O_4/PET nanoparticle films, the magnetic properties of these materials can be affected by an external magnetic field. When one end of the film is fixed, the film will experience bending deformation perpendicular to its direction under the influence of the external magnetic field. The magnetic field was added from 0 mT to 100 mT, and when the magnetic field reached 70 mT, the film reached its maximum deformation. The results show that the film has a strong magnetic response, and the deformation of the film can be controlled by a small magnetic field.

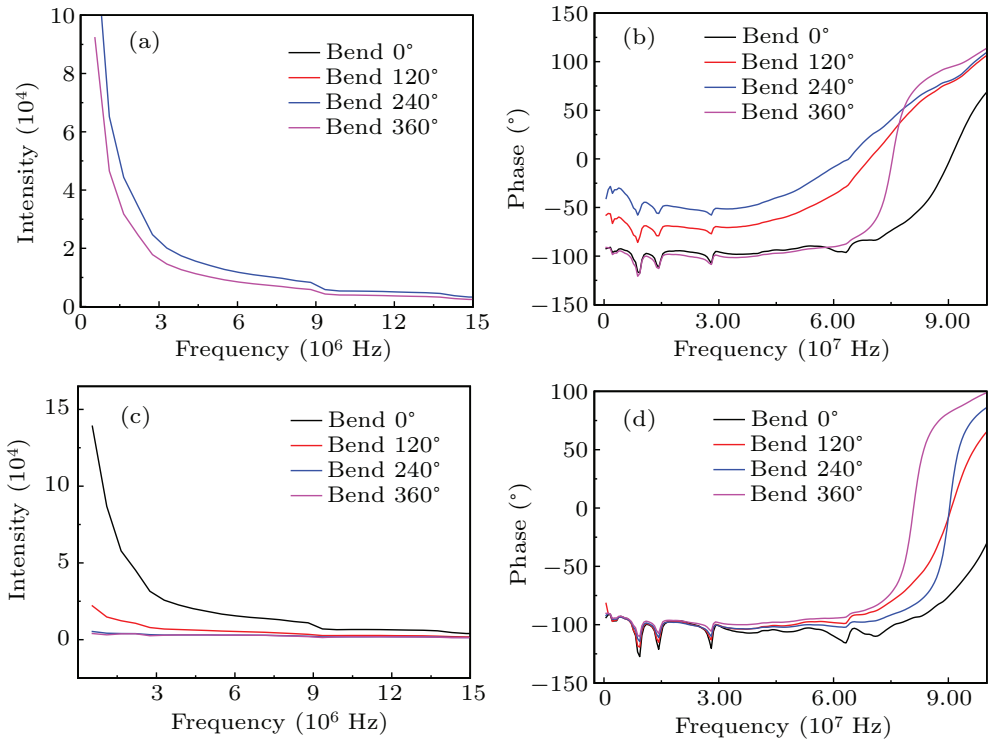


Fig. 5. The electrical properties of a flexible nanoparticle film bending at 0°, 120°, 240°, and 360°, respectively. (a) AC impedance of the assembled films from 40 Hz to 110 MHz without a magnetic field. (b) Phase angles of the assembled films without a magnetic field. (c) AC impedance of the assembled films with a 20 mT magnetic field. (d) Phase angles of the assembled films with a 20 mT magnetic field.

Due to the fact that thin films can be used as electromagnetic devices, the stress experiment of the film showed that the magnetic properties are mainly affected by the bending during the damage process;[22] therefore, the electric properties of the flexible assembled films were explored in the electromagnetic range from 40 Hz to 110 MHz with an impedance analyzer. The complex impedance amplitude of the flexible nanoparticle film frequency is plotted in Fig. 5(a). It was found that the amplitude of the impedance markedly reduced with increased bending of the film from 0° to 360°. Moreover, the phase angle exhibits a transition from negative to positive values in Fig. 5(b). This means that the assembled films became good electrical conductors. The conductivity of the nanoparticle film can be explained due to the enhancement of pathways for transporting electrons.[23] Because the flexible film is assembled from magnetic nanoparticles and has magnetism, we considered adding a 20 mT magnetic field and re-measuring the amplitude and phase angle (Fig. 5(c)). It was also found that the amplitude of the impedance reduced with an increase in the bending of the film. The impedance after bending was significantly reduced compared to that without the magnetic field. The results indicate that the ordered arrangement of magnetic moments was truly altered by the external magnetization. Thus, the ordered magnetic moment part enhanced the conductivity of the film. The change in the phase angle was not obvious in the range of 40–1 $\times$ 10^8 Hz, as seen in Fig. 5(d), indicating that the external magnetic field weakened the effect of bending on the conductivity of the flexible film.

During measurement of the electrical properties of thin films, the imaginary part of impedance and the phase angle change from negative to positive as the frequency increases. As shown in Figs. 5(b) and 5(d), the rapid increase in frequency occurs around 9×10^7 Hz. This may be due to the frequency reaching a threshold of the particle thin film, which then enhances its electrical properties. The conductivity of the film is significantly enhanced due to an increase in paths for transporting electrons. As a result, the film demonstrates high electrical conductivity.

3. Conclusion and perspectives

In summary, we fabricated a magnetoelastic nanoparticle Fe_3O_4 film on flexible PET substrates and observed a significant discrepancy in magnetocaloric effects upon deformation of the film. The measurement results showed that the film had magnetic anisotropy, and the assembled film had a magnetic enhancement effect. The contact angle and Raman results showed that the film's surface had excellent hydrophilicity and light absorption. With the noticeable change in deformation impedance, the film demonstrated a better magnetic response and electromagnetic characteristics. We believe that this nanoparticle film will be favorable for the development of biomedical materials with flexible magnetism.

Appendix A: Experimental details

A1. Magnetic nanoparticle synthesis

In the experiment, iron oxide nanoparticles were synthesized using the coprecipitation method. Firstly, $N(CH_3)_4OH$ was added to a mixture of $FeCl_2{\cdot}4H_2O$ and $FeCl_3{\cdot}6H_2O$ (in a molar ratio of 1:2), which had been dissolved in ultra-pure water in an alkaline environment. Then, ammonium hydroxide was slowly added to the mixed solution. The solution was heated to 70–80 °C for half an hour with stirring at 500 rpm during this process. Secondly, polydextrose sorbitol carboxyl methyl ether was dissolved in moderate ultra-pure water and added to the reaction flask. After heating for 0.5 h, the colloidal suspension was magnetically separated and washed with ultra-pure water three times. The whole synthesis process was conducted in a nitrogen atmosphere. After cooling to room temperature, the nanoparticles were washed twice with ultra-pure water to remove any redundant impurities. Finally, the products were collected via magnetic separation and dispersed in water. The temperature experiment was conducted in a low-preparation environment.

A2. Film assembly

The nanoparticle films were assembled layer-by-layer using a self-assembly method. Firstly, a piece of elastic transparent material, polyethylene terephthalate (PET), was cut to a size of 3 mm×5 mm. The material was plasma-treated to remove organic pollutants and oxides from the object's surface. Then, the elastic film was dipped into a 20 wt% poly-dimethyldiallyl ammonium (PDDA) chloride solution for 15 min. Next, the film was dried using a stream of nitrogen gas after washing with ultra-pure water. Then, the PET film was dipped into a Fe_3O_4 colloidal suspension for 15 min. The PET film with nanoparticles on the surface was then dried using a stream of nitrogen gas after washing with ultra-pure water. A multi-layered film of nanoparticles could be fabricated by repeating this process. In the experiment, 60 layers were assembled. Magnetothermal measurements were then taken.

In the magnetic thermal measurement section, the magnetic nanoparticle PET film was subjected to an alternating magnetic field for measurement of bending-dependent magnetothermogenesis. The film was bent 0°, 120°, 240°, and 360° respectively. The measurement process in the experiments continued for 15 min and the temperature was recorded by an optical fiber sensor and data recorder. Transmission electron microscopy (TEM) was performed using a JEM-2100 (Japan) system. Scanning electron microscopy (SEM) was carried out using a Zeiss Supra 40 Gemini (Germany) system.

The thermogenesis of magnetic hydrogel was measured using a fiber spectrometer (FISO UMI 8, Canada) and a thermal imager (Fluke, TI32). The magnetization of the samples was measured using VSM (model 7407, Lake Shore Cryotronics, Inc., USA). The electrical properties of the flexible nanoparticle film were measured using an impedance analyzer (Agilent 4294A, China). Morphological characterization was performed using atomic force microscopy (AFM, 5500AFM/STM, China).

Acknowledgements

Project supported by Scientific Research Funds (Grant No. 7001/700199) and Henan Provincial Department Scientific Research Project (Grant No. 22A430034).

References

[1] ia Y P, Ling Z G and Pan H L 2023 *Chin. Phys. B* **32** 027501
[2] Soriano D, Katsnelson M I and Fernandez-Rossier J 2020 *Nano Lett.* **20** 6225
[3] Jiang W, Hou Y F, Li S J, Fu Z G and Zhang P 2021 *Chin. Phys. B* **30** 127501
[4] Hu L B, David S H and Grüner G 2010 *Chem. Rev.* **110** 5790
[5] Zhao X, Wang K and Li B 2018 *Anal. Chemi.* **90** 7158
[6] Tyle R R, Jungil C, Bandodkar A J, Siddharth K, Philipp G, Limei T, Roozbeh G and John A R 2019 *Chem. Rev.* **119** 5461
[7] Loong L M, Lee W and Qiu X 2016 *Adv. Mater.* **28** 4983
[8] Liu W, Liu M and Ma R 2018 *Adv. Funct. Mater.* **28** 1705928
[9] Yong Z, Ming L and Shen L 2017 *ACS Nano* **11** 8002
[10] Merabtine S, Zighem F and Garcia-Sanchez A 2018 *Sci. Rep.-UK* **8** 13695
[11] Zighem F, Bahoui A E and Moulin J 2014 *J. Appl. Phys.* **116** 1062
[12] Sun X, Bedoya-Pinto A and Llopis R 2014 *Appl. Phys. Lett.* **105** 083302
[13] Kozakova Z, Kuritka I, Kazantseva E N, Babayan V, Pastorek M, Machovsky M, Bazant P and Saha P 2015 *Dalton T.* **44** 21099
[14] Nabiyouni G, Julaee M, Ghanbari D, Aliabadi P C and Safaie N 2015 *J. Ind. Eng. Chem.* **21** 599
[15] Xie J, Zhang Y and Yan C 2014 *Biomaterials* **35** 9126
[16] Chen B, Sun J and Fan F 2018 *Nanoscale* **10** 7369
[17] Li Y, Hu K and Chen B 2017 *Colloid. Surface. A* **520** 348
[18] Fan F, Sun J and Chen B 2018 *Sci. China. Mater.* **61** 1
[19] Merabtine S, Zighem F, Garcia-Sanchez A 2018 *Sci. Rep.-UK* **8** 13695
[20] Ochiai E I 1978 *J. Chem. Educ.* **55** 631
[21] Mohammeda D W, Ameena R B, Sierros K A, Bowenc J and Kukureka S N 2018 *Thin Solid Films* **645** 241
[22] Dai G, Zhan Q and Liu Y 2012 *Appl. Phy. Lett.* **100** 3238
[23] Sun J, Fan F and Wang P 2016 *Chemphyschem.* **17** 3377